CYCLIC TESTING OF STEEL MOMENT CONNECTIONS REHABILITATED WITH RBS OR WELDED HAUNCH

By Chia-Ming Uang,[1] Member, ASCE, Qi-Song "Kent" Yu,[2] Student Member, ASCE, Shane Noel,[3] and John Gross,[4] Members, ASCE

ABSTRACT: The effectiveness of using the reduced beam section (RBS) and welded haunch for seismic rehabilitation of pre-Northridge steel moment connections was investigated through cyclic testing of six full-scale specimens—three of them incorporated lightweight concrete slabs. Test results showed that, unless the low-toughness E70T-4 groove weld was replaced by notch-tough weld metal, introducing RBS to the beam bottom flange alone could not prevent brittle fracture in the groove weld of the top flange. The presence of a concrete slab or removing steel backing only improved the cyclic performance slightly. Although two RBS specimens with weld replacement performed well, a new type of ductile fracture along the "k" line of the beam was observed. With E70T-4 groove welds in place, however, the welded haunch specimens performed better than the RBS specimens. No brittle fracture occurred when the slab was present. The composite slab only increased the beam positive flexural strength by about 10%.

INTRODUCTION

Steel special moment-resisting frames (SMRFs), believed to be capable of dependable and ductile response during strong earthquake shaking, have long been considered a premier lateral force-resisting system. Because SMRFs provided large unobstructed spaces, this type of framing system was very popular in high seismic regions of the United States. For more than two decades, design engineers have used an economical bolted web-welded flange moment connection for this type of system. Unfortunately, brittle fracture in or around the groove weld between the beam flanges (primarily bottom flange) and the column flange was observed in more than 150 steel SMRF buildings after the January 17, 1994 Northridge earthquake (Youssef et al. 1995).

The widespread occurrence of these connection failures clearly demonstrated the fundamental deficiencies of steel SMRF design and construction practice prior to the Northridge earthquake. Among the concerns regarding the poor performance of these connections is the ability to effectively and economically rehabilitate steel moment connections in existing buildings. In response to this need, an experimental research program was funded by NIST, Gaithersbury, Md., and AISC, Chicago. This paper summarizes major findings of the project conducted at the University of California, San Diego (Yu et al. 1997). A parallel research project to test specimens with smaller member sizes was conducted at the University of Texas, Austin (Civjan and Engelhardt 1998).

[1]Assoc. Prof., Dept. of Struct. Engrg., Univ. of Calif. at San Diego, La Jolla, CA 92093-0085.

[2]Grad. Res. Asst., Dept. of Struct. Engrg., Univ. of Calif. at San Diego, La Jolla, CA.

[3]Des. Engr., Degenkolb Engineers, San Francisco, CA 94104; formerly, Grad. Res. Asst., Univ. of California at San Diego, La Jolla, CA.

[4]Build. and Fire Res. Lab., Nat. Inst. of Standards and Technol., Gaithersburg, MD 20899.

Note. Associate Editor: Takeru Igusa. Discussion open until June 1, 2000. Separate discussions should be submitted for the individual papers in this symposium. To extend the closing date one month, a written request must be filed with the ASCE Manager of Journals. The manuscript for this paper was submitted for review and possible publication on March 2, 1999. This paper is part of the ***Journal of Structural Engineering***, Vol. 126, No. 1, January, 2000. ©ASCE, ISSN 0733-9445/00/0001-0057–0068/$8.00 + $.50 per page. Paper No. 20491.

REHABILITATION SCHEMES AND DESIGN CONSIDERATIONS

Major Causes of Poor Performance of Pre-Northridge Moment Connections

According to a damage survey (Youssef et al. 1995), about 70–80% of the reported damage occurred in the beam bottom flange. Reasons for the dominance of bottom flange fractures in these connections that were designed in accordance with the *Uniform building code* (UBC) (1985, 1988) and constructed prior to the Northridge earthquake have been reported (SAC 1996a). First, it was recognized after the Northridge earthquake that the beam flange groove weld made with a low-toughness electrode (e.g., E70T-4) is prone to brittle fracture. Bottom flange is more likely to experience fracture because the groove weld cannot be made continuously across the flange width due to the interference of the beam web. Second, it is now understood that the incomplete fusion zone at the root pass of the weld would inevitably create a notch-like condition when steel backing is left in position. The location of the notch coincides with the extreme fiber location of the beam bottom flange. However, this is not the case at the beam top flange. Third, the concrete floor slab may have increased the positive flexural capacity, raising the beam neutral axis and, therefore, creating a larger tensile strain in the bottom flange.

Two Rehabilitation Schemes

RBS Scheme

A portion of the beam near the column was weakened in the reduced beam section (RBS) scheme so that plastic hinging would occur at the designated location. Seismic design of steel SMRFs is generally governed by code-prescribed drift limitations; that is, stiffness, not strength, dictates the member sizes. Therefore, member sizes that are selected for the drift requirement can be significantly larger than those required to satisfy the code strength requirement. Because of this member-size overstrength, weakening of the beams is feasible for steel SMRFs. Introducing a "structural fuse" with a reduced beam flange width near the beam-column connection has little effect on the beam or overall lateral stiffness, but the flange force that can be transmitted to the connection is reduced. Reducing the beam moment capacity also provides the following advantages: (1) The shear force in the panel zone is reduced; (2) the

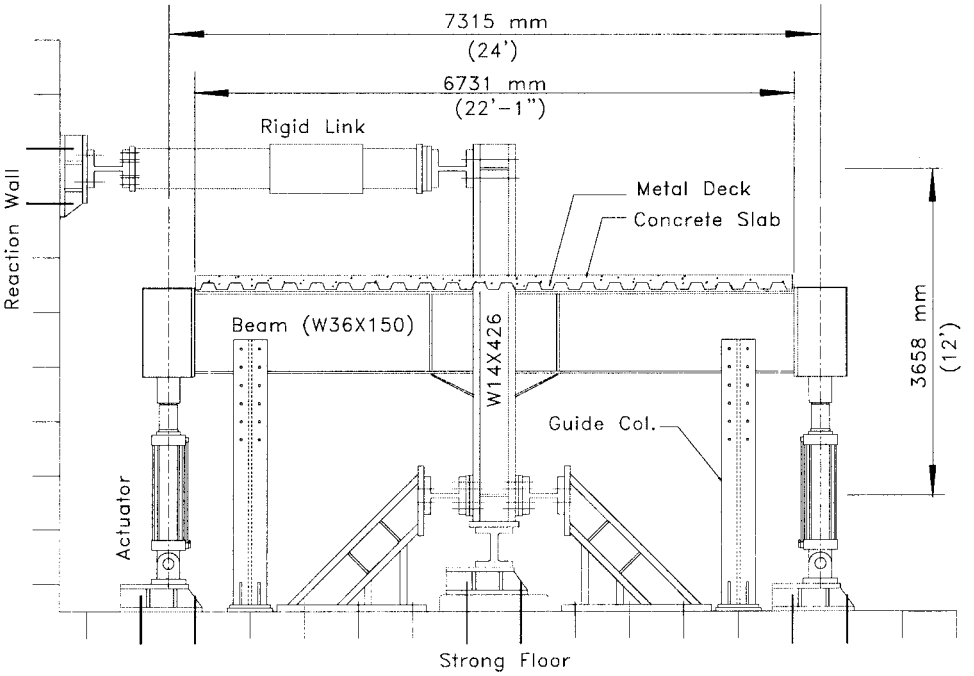

FIG. 1. Test Setup

TABLE 1. Steel Material Characteristics

Member (1)	Steel grade (2)	Location (3)	Yield strength[a] (MPa) (4)	Tensile strength[a] (MPa) (5)	Elongation[b] (%) (6)
Beam (W36×150)	A36	Flange	338 (49.0)	476 (69.0)	25
		Web	328 (47.5)	452 (65.5)	34
Column (W14×426)	A572 Grade 50	Flange	—	—	—
		Web	421 (61.0)	540 (78.3)	27
Haunch (W18×143)	A572 Grade 50	Flange	407 (59.1)	503 (73.0)	30
		Web	378 (54.8)	494 (71.6)	27

[a]Values in parentheses are in ksi.
[b]Elongation is based on 203 mm (8 in.) gauge length.

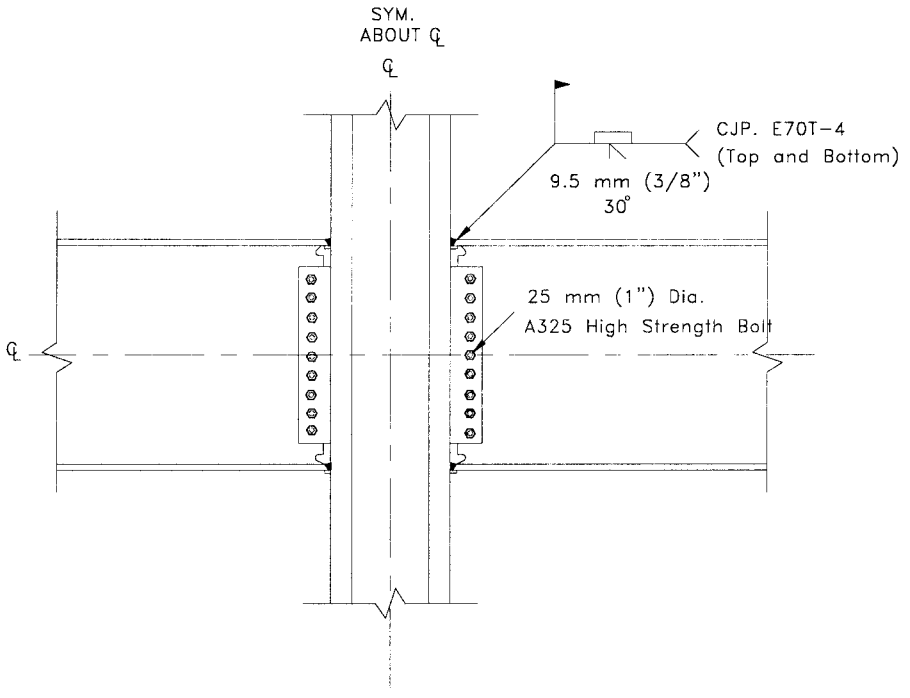

FIG. 2. Pre-Northridge Moment Connection Details

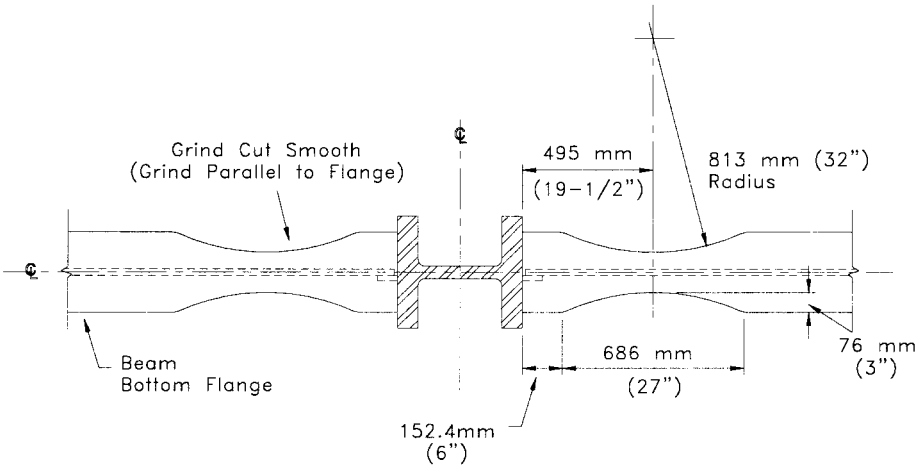

FIG. 3. Plan Views of RBS Connection (RBS at Bottom Flange Only)

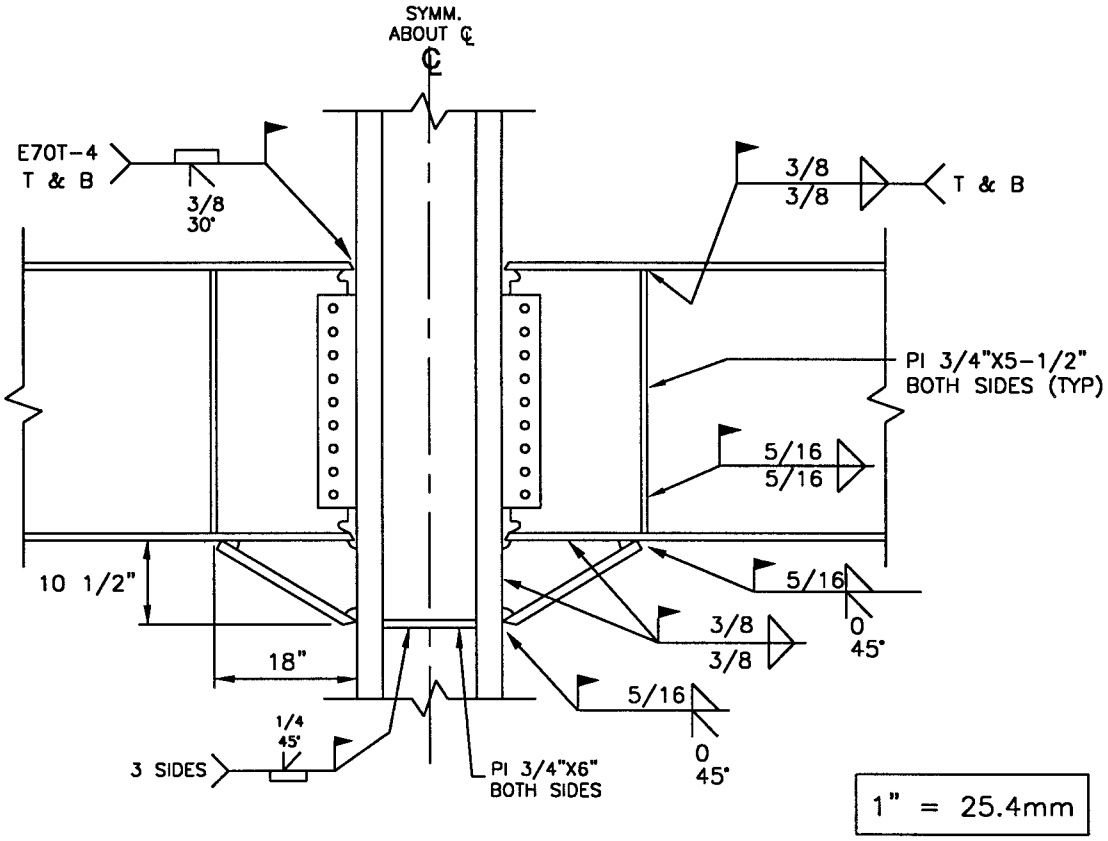

FIG. 4. Details of Welded Haunch Connection

force demand in column continuity plates is reduced; and (3) the weak beam-strong column requirement is easier to satisfy.

Welded Haunch Scheme

The second scheme was to strengthen the steel beam near the welded connection by welding a triangular haunch beneath the beam bottom flange. Ideally, the strengthened section of the beam would remain primarily elastic during plastic hinging of the beam, thereby limiting the stress in the welds. Because the beam reaches its full plastic moment away from the column face, this type of reinforced connection is subjected to a higher moment than the RBS connection.

Other Considerations

Although both methods attempt to achieve the desired performance by reducing the stress in the beam flange groove weld, the quality of the groove weld also needs to be considered. Since the Northridge earthquake, for new construction, beam flange groove welds generally have been specified to use an electrode with a specified Charpy V-notch toughness, say 27.1 J (20 ft-lb) at −28.8°C (−20°F) (SAC 1996a). To modify existing moment connections, however, it is highly desirable to minimize the amount of work required to modify (or even replace) the existing low-toughness groove welded joint for economical reasons.

The concrete slab in existing buildings presents another problem for economic considerations in seismic rehabilitation projects. Unless the concrete slab around the column is removed, it is difficult to modify the top flange and its welded joint. Because the majority of reported damage occurred in the bottom flange, it was speculated that modifying only the bottom flange may be sufficient to significantly improve the performance of the connections.

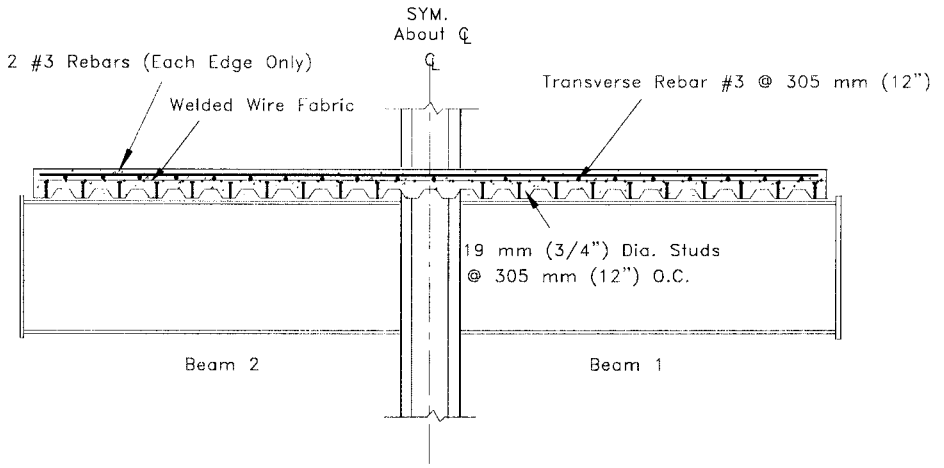

FIG. 5. Composite Slab Details

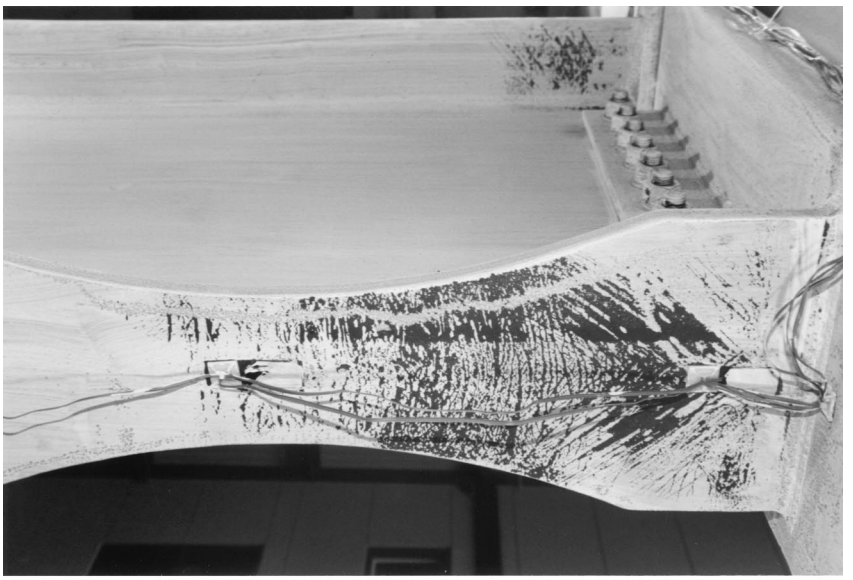

(a)

(b)

FIG. 6. Yielding Pattern and Fracture of Beam 2 (NIST-1): (a) Yielding Pattern; (b) Brittle Fracture of Top Flange Welded Joint

RESEARCH OBJECTIVES AND SCOPE

The main objective of this research was to investigate the effectiveness of using either the RBS or welded haunch technique for the seismic rehabilitation of pre-Northridge steel moment connections. For either of the rehabilitation schemes, an attempt was made to modify only the beam bottom flange and its welded joint. Three sets of full-scale specimens (two specimens for each set) with two-sided moment connections were tested. One of the two specimens in each set incorporated a lightweight concrete slab. The first set (Specimens NIST-1 and NIST-1C, where ''C'' refers to the specimen with a concrete slab) and third set (Specimens NIST-3 and NIST-3C) of specimens incorporated RBS. The second set (Specimens NIST-2 and NIST-2C) of specimens incorporated a welded haunch.

DESCRIPTION OF TEST SPECIMENS

The specimen geometry and overall test setup are shown in Fig. 1. The geometry of the test specimens was chosen to model the interior connection of a multistory steel frame with a 3,658-mm (12-ft) story height and 7,315-mm (24-ft) bay width. All six nominally identical steel beam-to-column subassemblies were first constructed for rehabilitation. Each specimen consisted of one W14×426 (A572, Grade 50 steel) column and one W36×150 (A36 steel) beam on each side of the column (see Table 1 for material properties). The pre-Northridge moment connections (Fig. 2) were designed in accordance with UBC (1985).

Each specimen was constructed and inspected using techniques similar to those used in pre-Northridge construction. Beam flange groove welding was performed with a 3.05 mm (0.12 in.) diameter E70T-4 electrode (Lincoln NS-3M) with steel backing and weld tabs left in place. Slip-critical A325 high-strength [diameter = 22 mm (7/8 in.)] with a specified minimum pretension force of 169 kN (39 kips) were fully tightened using the turn-of-nut method. Modification of these pre-Northridge moment connections then proceeded after these moment connections passed ultrasonic testing. A 1.8 mm (0.072 in.) diameter E71T-8 electrode (Lincoln NR-232) with a specified Charpy V-notch toughness of 27.1 J (20 ft-lb) at

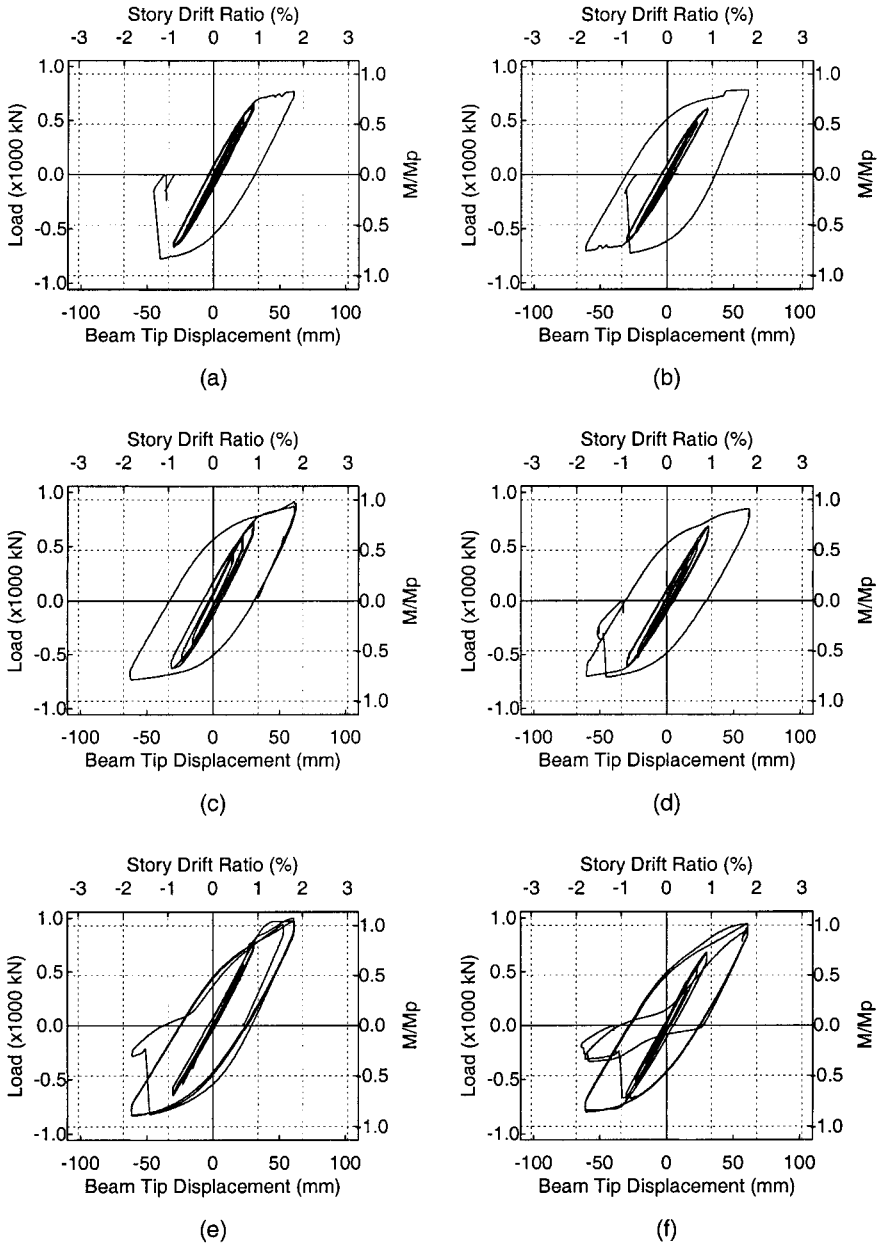

FIG. 7. Load versus Displacement Relationships of RBS Specimens: (a) Beam 1 of NIST-1; (b) Beam 2 of NIST-1; (c) Beam 1 of NIST-1C; (d) Beam 2 of NIST-1C; (e) Beam 1 of NIST-1C-R; (f) Beam 2 of NIST-1C-R

−28.8°C (−20°F) was used for making all the welds for connection modifications.

Modification Design and Details of RBS Connections

Fig. 3 shows the geometry of the RBS that was introduced to the beam bottom flanges of the first and third sets of specimens. The test specimens had a 50% reduction in the beam bottom flange, resulting in a reduction of the plastic section modulus by 19%. Assuming that the plastic hinge would form at the narrowest section and that the strain-hardening factor is 1.1 (SAC 1996a), the moment at the face of the column can be computed by extrapolation to be 1.04 of the beam nominal plastic moment M_{pn}.

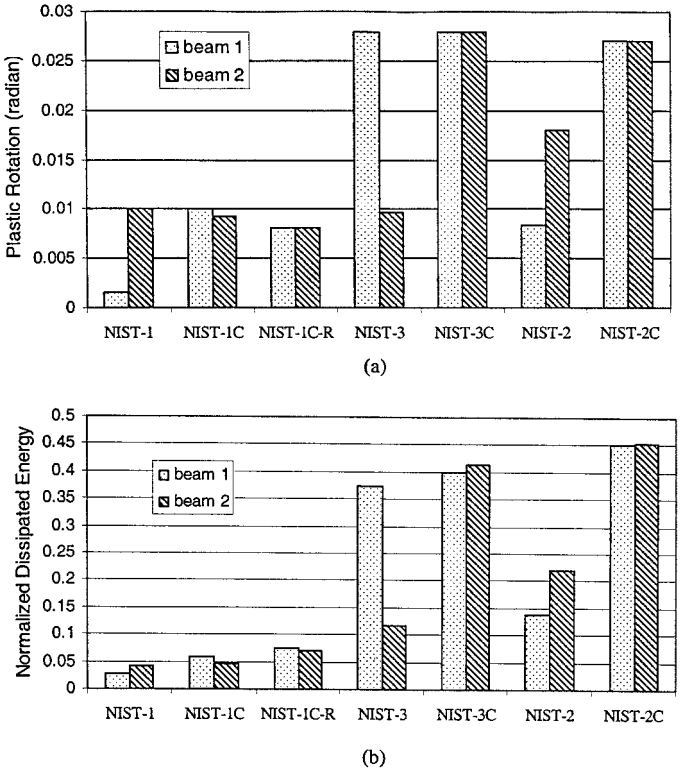

FIG. 8. Comparison of Plastic Rotation and Energy Dissipation Capacities: (a) Plastic Rotation; (b) Normalized Energy Dissipation

Steel backing and weld tabs of the bottom flange groove weld were removed. The exposed root pass was first back-gouged to sound metal. The gouged portion was then refilled with new weld metal before a 16 mm (5/8 in.) reinforcing fillet weld was applied beneath it.

Modification Design and Details of Welded Haunch Connections

Fig. 4 shows the geometry and welding details of the haunch that was welded to the second set of specimens. In the SAC Phase I program, two damaged pre-Northridge moment connections with the same beam size (W36×150) that were repaired by the welded haunch performed well under cyclic loading (SAC 1996b). It was then decided to use the same haunch size and geometry in this test program. No modification was made to the existing top flange groove welded joints.

Composite Slab Details

The design and construction of the concrete slab were chosen to reflect a common practice of composite floor slab construction in California. (Beams in SMRFs are typically not designed as composite beams.) A 2,438 mm (8 ft) wide lightweight concrete slab was incorporated in three specimens. The details for the concrete slab construction are shown in Fig. 5. The slab width on each side of the beam corresponded to one-sixth the beam span. The 76 mm (3 in.) deep corrugated metal deck (BHP 3W-36, gauge 20, zinc coated, ASTM A446, Grade A) was oriented such that the flute was perpendicular to the longitudinal direction of the beams. Nelson headed shear studs, 140 mm (5.5 in.) long, 19 mm (0.75 in.) in diameter, were fillet welded 305 mm (12 in.) on center to the beam top flange along the beam centerline. The shear capacity of these headed studs created a partial composite action corresponding to 12% of the full composite action.

The slab consisted of 83-mm (3.25-in.) lightweight concrete [f'_c = 34.5 MPa (5 ksi)] fill on top of the steel deck. The slab reinforcement consisted of a welded wire fabric (6×6-W1.4×W1.4) and No. 3 steel reinforcements (Grade 60) placed transversely at 305 mm (12 in.) on center. To control the wide crack in the slab that was observed after testing NIST-1C, two No. 3 reinforcing bars were placed longitudinally along the edges of the slab for Specimens NIST-2C and NIST-3C.

FIG. 9. Failure Mode of NIST-3C

TEST PROCEDURE AND DATA REDUCTION PROCEDURE

The ATC-24 (ATC 1992) testing protocol was used for the tests. The loading protocol calls for three cycles at $0.5\delta_y$, $0.75\delta_y$, $1\delta_y$, $2\delta_y$, $3\delta_y$ displacement amplitudes, respectively, which are then followed by two cycles at $4\delta_y$, $5\delta_y$, etc. For testing purposes, a controlling value of δ_y equal to 30 mm (1.2 in.) was used for all the test specimens. The testing was conducted quasi-statically in a displacement-controlled mode (i.e., equal and opposite displacements were applied to the cantilever end of the beams). The positive displacement was defined as Beam 1 displacing upward while Beam 2 displaced downward.

The procedures for computing the plastic rotations of the test specimens with and without haunches were similar to those described by Uang and Bondad (1996). The Acceptance Criteria in Section 7.4.2 of the SAC Interim Guidelines (SAC 1996a) was adopted for determining the plastic rotation.

CYCLIC BEHAVIOR OF RBS SPECIMENS

RBS Specimens: NIST-1 and NIST-1C

General Behavior and Failure Mode

The yielding pattern and failure mode of both specimens were very similar. Significant yielding was observed during the $2\delta_y$ cycles [story drift ratio (SDR) = 1.7%]. Yielding of beam bottom flanges extended from the column face to the narrowest beam section [Fig. 6(a)], but yielding of the top flange was confined in a narrow region next to the column face. Beam 1 of NIST-1 experienced brittle fracture before the first cycle of $2\delta_y$ was completed. Beam 2 suffered a similar fracture during the next excursion after Beam 1 was unloaded and held at a constant displacement [Fig. 6(b)]. The presence of a concrete slab in NIST-1C delayed the beam fracture, which first occurred in Beam 2, by a half-cycle. Brittle fracture of both specimens occurred in the weld metal of beam top flanges; no beam buckling was observed.

Once improvement was made to the beam bottom flange, it became obvious from the test results of both NIST-1 and NIST-1C that the existing top flange groove welded joints were vulnerable to brittle fracture, irrespective of the presence of a concrete slab. It was speculated that removing steel backing of the top flange groove weld joint might have improved the cyclic performance. Therefore, it was decided to repair and restore the damaged top flange of NIST-1C to the pre-Northridge condition first, which was then followed by removing steel backing for retesting. The repair involved the following steps: (1) Remove a portion of the concrete slab around the column for access; (2) replace the fractured weld with new weld metal deposited with the same electrode (E70T-4); (3) remove steel backing and weld tabs and then apply a reinforcing fillet weld after the root pass is backgouged and refilled; and (4) patch the cut portion of the slab with concrete. Because ultrasonic testing revealed no rejectable defects in the top flange welded joint of Beam 1, only Step 3 was used for the modification. The repaired specimen was designated as NIST-1C-R.

Retesting of NIST-1C-R demonstrated that removing steel backing and weld tabs of top flanges delayed brittle fracture by only another half-cycle in the $2\delta_y$ cycles. The newly deposited groove weld in the top flange of Beam 2 fractured near the completion of the second cycle, which was followed by a similar fracture in the top flange of Beam 1. No fracture occurred in the bottom flange welded joints in all three tests, indicating that the RBS and measures to eliminate the notch-like condition were effective in protecting the bottom flange groove welded joints.

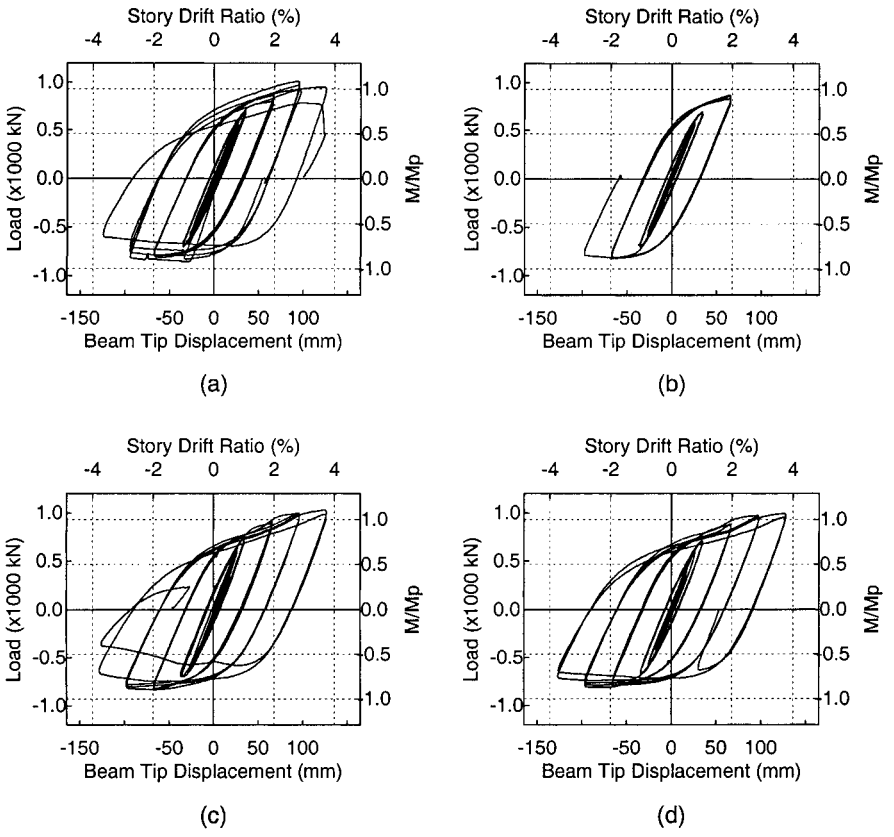

FIG. 10. Load versus Displacement Relationships of Improved RBS Specimens: (a) Beam 1 of NIST-3; (b) Beam 2 of NIST-3; (c) Beam 1 of NIST-3C; (d) Beam 2 of NIST-3C

Measured Response

Load versus beam tip displacement relationships for all three tests are shown in Fig. 7. Inelastic deformation occurred mainly in the steel beams, whereas yielding in the panel zone and the column was very limited. These plots include a normalized moment axis, where M is the moment at the column face, and M_p is the full-section plastic moment of the beam based on the actual yield stresses. Note the strength of NIST-1C-R was about 10% higher than that of NIST-1C. Because beams of NIST-1C-R experienced prior yielding during the test of NIST-1C, and NIST-1C-R was tested 4 months later, the increase in strength might have been caused by strain aging of the steel (Salmon and Johnson 1996).

Plastic rotations based on the centerline dimensions are summarized in Fig. 8(a). The maximum plastic rotation capacity developed in this set of specimens was about 0.01 rad. A similar comparison for the energy dissipation capacities, normalized by M_p, is shown in Fig. 8(b). (The normalized energy dissipation is a measure of the cumulative plastic rotation capacity.)

Improved RBS Specimens: NIST-3 and NIST-3C

This set of specimens had the same RBS configuration as the first set of specimens, but the existing groove welds in both flanges were removed and then rewelded with an E71T-8 electrode. All steel backing and weld tabs were also removed.

General Behavior and Failure Mode

The performance of this set of specimens was significantly improved. Brittle fracture of the welded joints did not occur, but a new mode of ductile fracture was observed. Local buckling was first observed in the lower portion of the beam web during the $2\delta_y$ cycles, which was then followed by lateral-torsional buckling in the RBS region of the beams. Ductile tearing originating from the beam flange weld access hole due to stress concentration and propagating along the ''k'' line of the beam (i.e., near the junction of the beam web and the beam flange) was observed. Fig. 9 shows the fracture mode in NIST-3C during the $4\delta_y$ cycles. A fracture of 191 mm (7.5 in.) in length separated the beam bottom flange from the web of

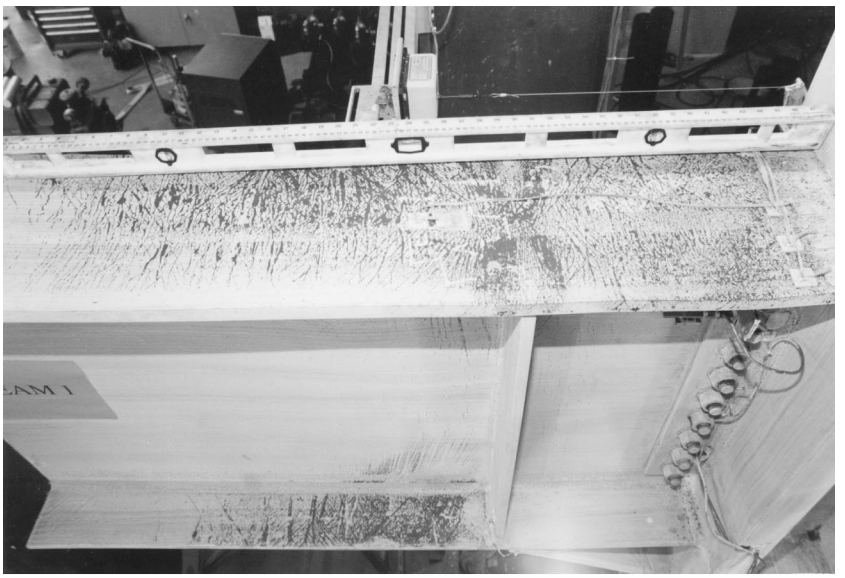

(a)

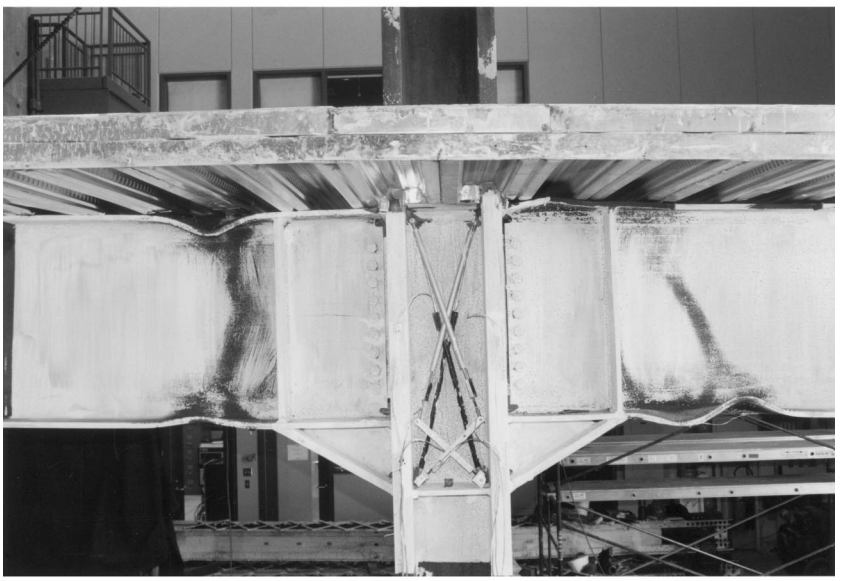

(b)

FIG. 11. Buckling and Yielding Modes of Welded Haunch Specimens: (a) NIST-2; (b) NIST-2C

Beam 1 during the second positive excursion of $4\delta_y$ cycles. When the direction of loading was reversed, the figure shows that the separated bottom flange buckled away from the beam web like a compression member, causing a drastic drop of beam strength by 60%.

Measured Response

Fig. 10 shows the load versus beam tip displacement relationships for both specimens. Note that the cyclic performance of Beam 2 in NIST-3 was poor. It was observed that the top flange of this beam was not properly braced for lateral movement during testing. Significant twisting of this beam caused the fracture that initiated at the weld access hole to rapidly propagate into the bottom flange. The significant strength reduction of Beam 1 during the last negative excursion of NIST-3C was caused by the failure mode shown in Fig. 9. Except for this last excursion, strength degradation, which was caused primarily by buckling in the RBS region, in other negative excursions was minor.

The plastic rotation and energy dissipation capacities of these specimens are summarized in Figs. 9 and 10, respectively. Except for Beam 2 of NIST-3, the cyclic performance was significantly better than that of the first set of specimens.

CYCLIC BEHAVIOR OF WELDED HAUNCH SPECIMENS (NIST-2 AND NIST-2C)

General Behavior and Failure Mode

Significant yielding of NIST-2 occurred during the $2\delta_y$ cycles. From the flaking pattern of the whitewash, Fig. 11(a) shows that yielding of the bottom flange occurred outside the haunch region, and a much longer yielded length was developed in the top flange. Buckling of beams occurred during the $3\delta_y$ (SDR = 2.5%) cycles. Nevertheless, the groove weld of Beam 1 top flange fractured in the first negative excursion. The top flange of Beam 2 also experienced a similar weld fracture in the next positive excursion.

Specimen NIST-2C exhibited excellent performance. Both beams were able to complete the $4\delta_y$ (SDR = 3.3%) cycles without fracturing [Fig. 11(b)]. Both flanges of the beams experienced local buckling. However, the buckling amplitude of top flanges was smaller due to the presence of the concrete slab.

Measured Response

Load versus beam tip displacement relationships for both specimens are shown in Fig. 12. The gradual strength degradation of Beam 2 in NIST-2 due to beam buckling was observed only in the second positive excursion of the $3\delta_y$ cycles. Two factors contributed to the early strength degradation. First, the yielded length of the top flange was longer [Fig. 11(a)]. Second, the unbraced length of the top flange was longer than that of the bottom flange because the haunch was effective in providing lateral bracing to the bottom flange. When a concrete slab was present, as in NIST-2C, the slab was effective in providing continuous lateral bracing to the beam top flange. Therefore, strength degradation occurred primarily in negative bending.

The plastic rotation and energy dissipation capacities of both specimens are summarized in Fig. 8. NIST-2C, without experiencing any fracture, delivered the best performance of all specimens tested.

Based on the rosette gauge measurements, shear strains in the upper and lower portions of the column panel zone, beam web, and haunch web are compared in Fig. 13. (Gauge readings of R7 at higher displacement amplitudes were affected by beam web buckling.) The figure shows that only the upper panel zone of the column was yielded. The shear strain in the beam web outside the haunch region is theoretically opposite in sign to the shear strain in the column panel zone. Never-

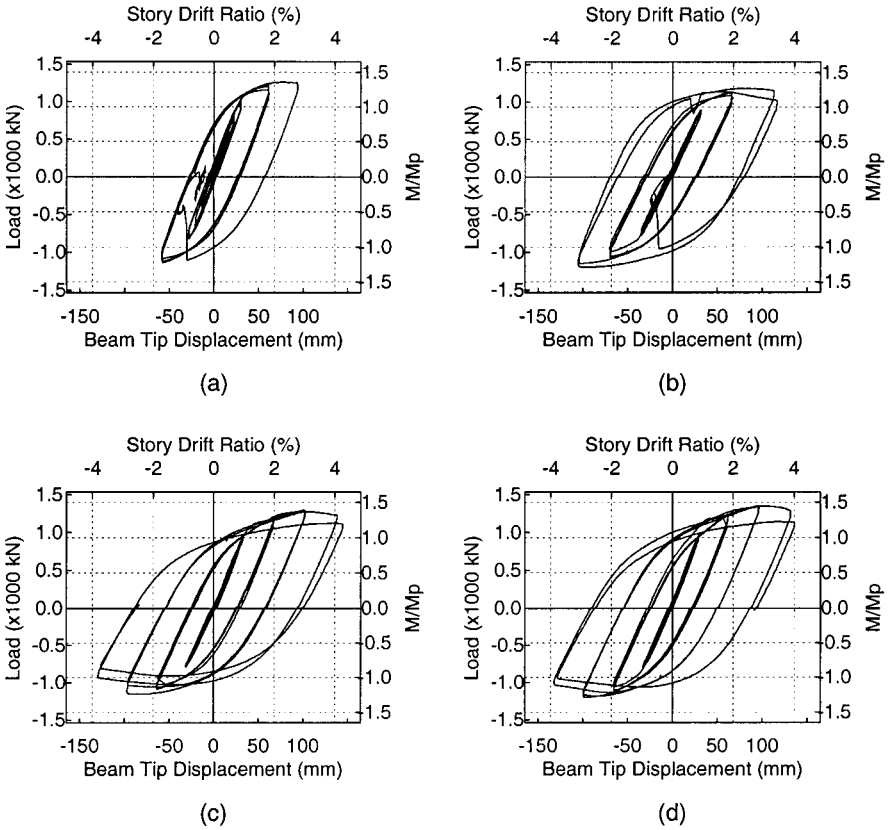

FIG. 12. Load versus Displacement Relationships of Welded Haunch Specimens: (a) Beam 1 of NIST-2; (b) Beam 2 of NIST-2; (c) Beam 1 of NIST-2C; (d) Beam 2 of NIST-2C

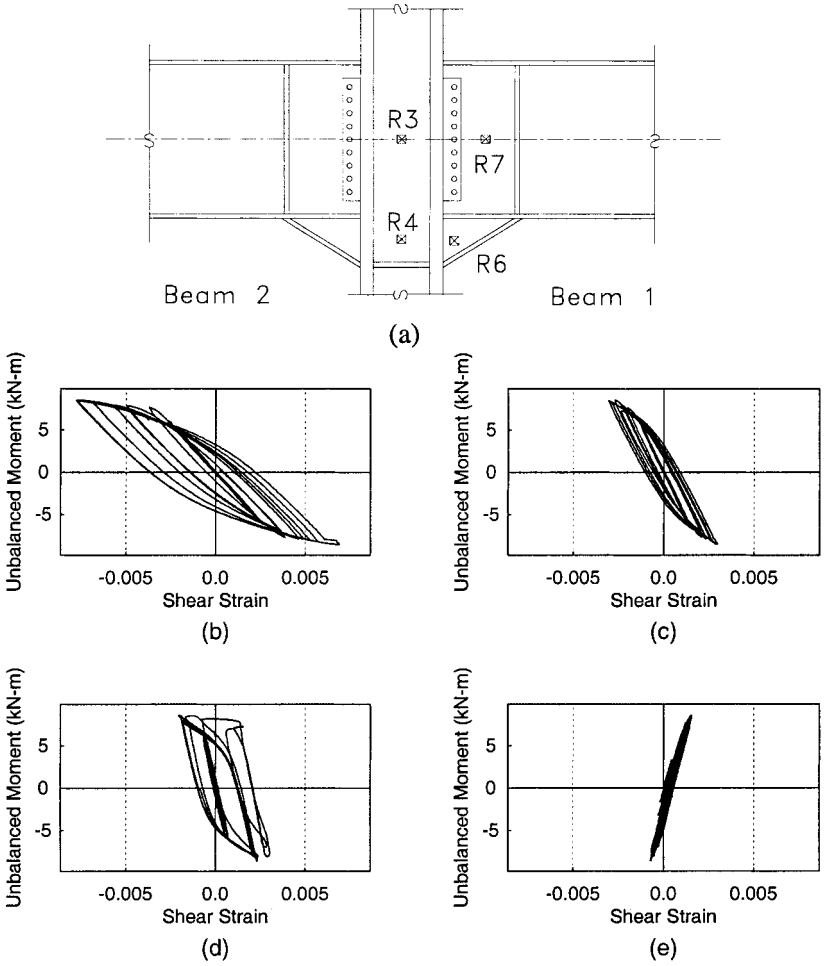

FIG. 13. Comparison of Shear Strains in Specimen NIST-2C: (a) Location of Strain Rosettes; (b) Upper Panel Zone—R3; (c) Lower Panel Zone—R4; (d) Beam Web—R7; (e) Haunch Web—R6

theless, the measurements indicated that the shear strain of the beam web in the haunch region had the same sign as that of the panel zone. The change of beam shear transfer mechanism and a reduction of the beam shear force in the haunch region were major contributing factors for the improved performance of haunch specimens. The implications of this observation for the haunch design are presented in the companion paper (Yu et al. 2000).

SLAB EFFECTS ON PERFORMANCE OF STEEL MOMENT CONNECTIONS

Slab Crack Patterns

The first cracking of the concrete slab occurred transversely at the column face. Concrete cracks were first observed when the displacement amplitude was as low as $0.25\delta_y$ (SDR = 0.21%), and these cracks extended across the entire width of the slab at $0.5\delta_y$ cycles. Because headed shear studs could provide only 12% of the full composite action, splitting of the concrete slab along the stud line was also observed during the $2\delta_y$ cycles, suggesting excessive slippage between the steel beams and the concrete slab. For NIST-2C, slippage on the order of 12.7 mm (0.5 in.) was recorded near the loaded beam end during the $3\delta_y$ displacement cycles.

Effective Width of Composite Slab

The wire mesh of each concrete slab was instrumented with strain gauges to construct strain profiles across the width of the slab; the measurements were made at a location 381 mm (15 in.) away from the face of the column. Fig. 14 shows such profiles for NIST-1C and NIST-2C. Under positive bending, the portion of concrete slab that was effective in developing compressive stresses was primarily confined in the width of column flange due to direct bearing between the column flange

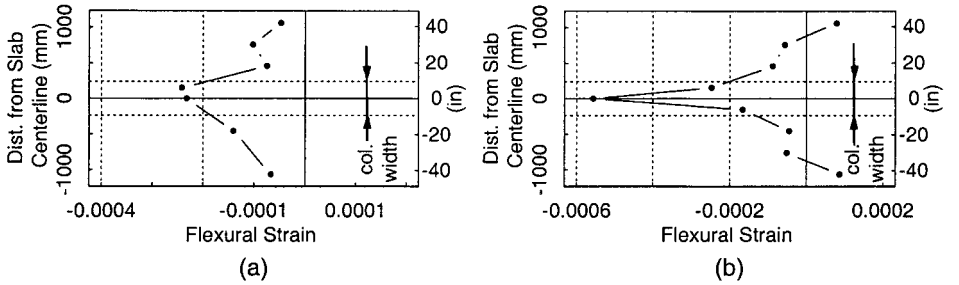

FIG. 14. Concrete Slab Compression Strain Profiles: (a) NIST-1C; (b) NIST-2C

and the concrete slab. Except for a small amount of inclined compression strut action that occurred just outside the column flange width, compressive stresses elsewhere were very low due to the presence of a wide, transverse concrete crack on the other side of the column, where the beam was in negative bending.

Strain Profiles along Beam Depth

The flexural strain profiles of NIST-2C along the depth of the steel beam are shown in Fig. 15. The location of measurements was 840 mm (33 in.) from the column. Under positive bending, Fig. 15(a) shows that the neutral axis was shifted slightly above the midheight of the steel beam due to the composite action. Fig. 15(b) shows that the neutral axis remained at the midheight of the steel beam under negative bending, which implied that the composite action was very limited.

Beam Buckling Modes

The concrete slab was effective in providing lateral bracing to the top flange so that lateral-torsional buckling would not occur under positive bending. But flange local buckling still could be developed [Fig. 11(b)]. Under negative bending, significant local buckling interacted with lateral-torsion buckling. The presence of a concrete slab had a negligible effect on the buckling mode. Thus, more significant strength degradation in negative bending was observed in the composite specimens.

Beam Flexural Strength

The effect of composite action on the beam flexural strength can be observed from the response envelopes shown in Fig. 16. For the haunch specimens, the flexural strength of composite beam under positive bending was slightly higher than that of steel beam (10% on average) for two reasons. First, composite action increased the flexural strength. Second, lateral bracing provided by the concrete slab eliminated lateral-torsional buckling. Although to a lesser extent, a similar level of increase of positive flexural strength was also observed in the RBS specimens. However, such an increase in flexural strength disappeared for composite beams under negative bending.

CONCLUSIONS

A total of six pre-Northridge two-sided steel moment frame connection specimens, each consisting of a W14×426 column (A572 Grade 50 steel) and two W36×150 beams (A36 steel), were tested cyclically to study the effectiveness of two seismic rehabilitation schemes: RBS and welded haunch. Three specimens incorporated a 2,438 mm (8 ft) wide lightweight concrete slab. The following conclusions can be made for the particular specimen sizes tested:

1. Introducing RBS to the beam bottom flange, which was accompanied by removing steel backing and weld tabs, could not prevent brittle fracture of the low-toughness groove welded joint in the top flange. The improvement of cyclic performance by either removing steel backing of the top flange or incorporating a concrete slab was marginal. The plastic rotation capacity was no more than 0.01 rad. This rehabilitation scheme was much more effective when the existing low-toughness groove welds (E70T-4) were replaced by those deposited with a notch-tough electrode (E71T-8). Brittle fracture of welded joints was precluded, but ductile tearing initiating from the beam flange weld access hole near the bottom flange and propagating horizontally along the ''k'' line of the beam was observed. Three of the four beams were able to develop a plastic rotation in excess of 0.027 rad.
2. Welding a triangular haunch to the beam bottom flange significantly improved the cyclic performance. Although welded joints of top flanges still suffered brittle fracture for the bare steel specimen, the specimen with a composite slab did not experience brittle fracture and was able to develop plastic rotations in excess of 0.027 rad.

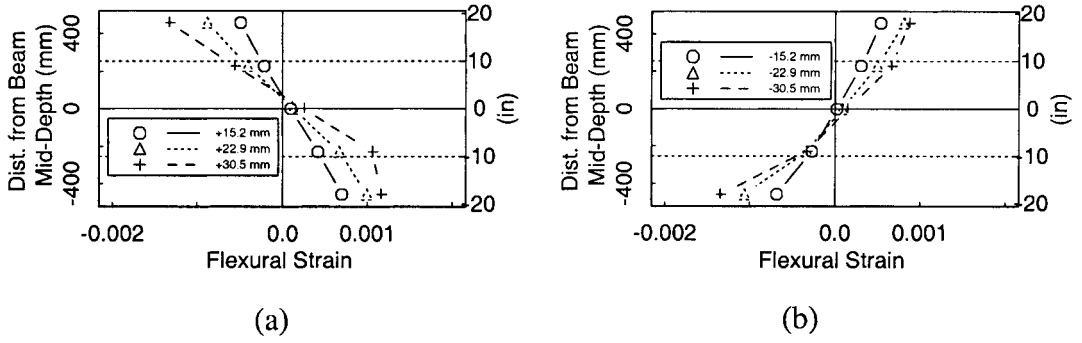

FIG. 15. Flexural Strain Profiles along Beam Depth of NIST-2C: (a) Positive Bending; (b) Negative Bending

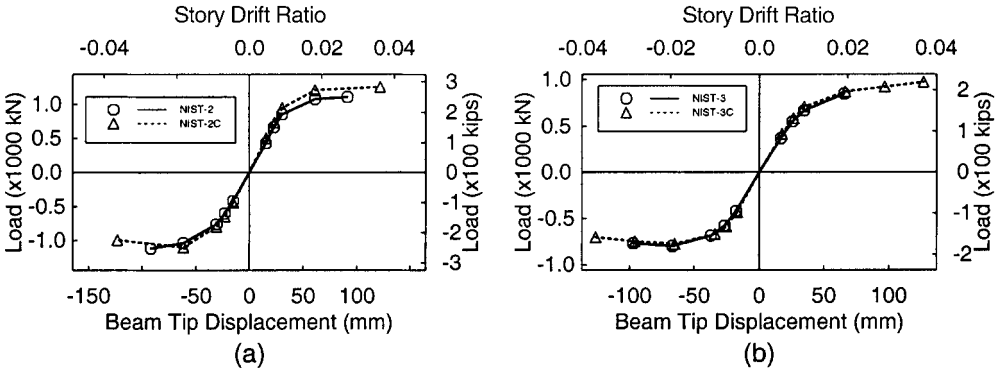

FIG. 16. Beam 2 Load versus Displacement Envelopes: (a) Haunch Specimens; (b) Improved RBS Specimens

This satisfactory performance was also confirmed by two additional tests in a parallel testing program (Civjan and Engelhardt 1998). An analytical model that can be used to explain the success of the welded haunch scheme is presented in the companion paper (Yu et al. 2000).

3. For the particular beam size (W36×150) tested, the presence of a 2,438 mm (8 ft) wide concrete slab increased the positive flexural strength of the beam by about 10% on average. No strength increase occurred in the negative bending direction, indicating that the concrete slab with welded wire mesh was not able to reduce the seismic force demand in the beam top flange. The presence of a concrete slab altered the beam buckling mode. Lateral-torsional buckling was prevented due to the bracing effect of the slab, but flange local buckling still could be developed under positive bending. Therefore, strength degradation due to buckling was less severe in positive bending than in negative bending.

ACKNOWLEDGMENTS

This research project was funded by the NIST, Gaithersburg, Md., (NIST) under Grant No. 70NANB5H0126. Additional financial support was provided through AISC, Chicago, by the Northridge Steel Industry Fund. The Structural Shapes Producers Council donated steel shapes and the Lincoln Electric Company donated welding electrodes. PDM/Strocal fabricated the test specimens at cost. Twinning Laboratories donated part of the nondestructive testing services. The writers also like to acknowledge Prof. M. D. Engelhardt, Prof. K. Kasai, A. Sadre, J. O. Malley, and P. M. Hassett for providing technical advice throughout the testing program.

APPENDIX. REFERENCES

ATC. (1992). ''Guidelines for cyclic seismic testing of components of steel structures for buildings.'' *Rep. No. ATC-24*, Applied Technology Council, Redwood City, Calif.

Civjan, S., and Engelhardt, M. D. (1998). ''Experimental investigation of methods to retrofit connections in existing seismic-resistant steel moment frames.'' *Summary Final Rep. to the National Institute of Standards and Technology*, Phil M. Ferguson Struct. Engrg. Lab., University of Texas at Austin, Austin, Tex.

Load and resistance factor design for structural steel buildings. (1993). American Institute of Steel Construction, Chicago, IL.

SAC. (1996a). ''Interim Guidelines Advisory No. 1.'' *Rep. No. SAC-96-03 (Rep. No. FEMA-267A*), SAC Joint Venture, Sacramento, Calif.

SAC. (1996b). ''Technical report: Experimental investigations of beam-column subassemblies.'' *Rep. No. SAC-96-01*, SAC Joint Venture, Sacramento, Calif.

Salmon, C. G., and Johnson, J. F. (1996). *Steel structures: Design and Behavior*, 4th Ed., HarperCollins, New York.

Uang, C.-M., and Bondad, D. (1996). ''Static cyclic testing of pre-Northridge and haunch repaired steel moment connections.'' *Rep. No. SSRP-96/02*, Div. of Struct. Engrg., University of California at San Diego, La Jolla, Calif.

Uniform building code. (1985). International Conference of Building Officials, Whittier, Calif.

Uniform building code. (1988). International Conference of Building Officials, Whittier, Calif.

Youssef, N., Bonowitz, D., and Gross, J. (1995). ''A survey of steel moment-resisting frame buildings affected by the 1994 Northridge earthquake.'' *Rep. No. NISTIR 5625*, NIST, Gaithersburg, Md.

Yu, Q.-S., Noel, S., and Uang, C.-M. (1997). ''Experimental and analytical studies on seismic rehabilitation of pre-Northridge steel moment connections: RBS and haunch approaches.'' *Rep. No. SSRP-97/08*, Div. of Struct. Engrg., University of California at San Diego, La Jolla, Calif.

Yu, Q.-S., Uang, C.-M., and Gross, J. (2000). ''Seismic rehabilitation design of steel moment connection with welded haunch.'' *J. Struct. Engrg*., ASCE, 126(1), 69–78.